

Commissioner for Patents

Serial No. 09/837,742

#### REMARKS

Claims 1 to 19 are in the case.

New claims 11 to 19 are presented depending from claims 6, 7 or 9 and reciting features found in claims 2, 3, 4 or 5 as filed.

#### Claim Rejections – 35 USC § 112

The preamble of each of claims 6 and 7 has been amended to broadly describe the known class of immuno-separation process and the known class of diagnostic method with which the present invention is concerned. These methods are part of the state of the art and described, for example, in the Rembaun et al publication, acknowledged at page 12 of the specification of the present application.

With the amendments made, the objection under 35 USC § 112 is believed to be overcome.

#### Claim Rejections – 35 USC § 102

Claim 1 stands rejected under 35 USC § 102 as being anticipated by Seiver et al.

Seiver et al is concerned with elongated ferromagnetic components for use in a fluidized bed. These ferromagnetic components are in the nature of elongated pellets. They have a particle size ranging from 10 micrometers to about 4000 micrometers with a length-to-diameter ratio of at least 2 but not more than 313, preferably not more than 30.

It is indicated that the "pellets" may be admixed with various gels and sols and set therein within a hydrogel matrix as pills, tablets, extrudates, beads or the like.

More especially, the pellets additionally include a catalyst.

The present invention is concerned with an altogether different class of composition and a different area of utility. Claim 1 has been amended in order to better distinguish over Seiver et al. In particular, claim 1 now recites that the particulate magnetic material has a particle size of 1 to 100 nm as taught at page 4, line 31. Claim 1 has further been amended to introduce therein the structural features set forth in original claim 5, namely, that the matrix is permeable and has accessible interior surfaces defining a cage for physical or chemical entrapment of an immuno-

Commissioner for Patents

Serial No. 09/837,742

reactant or diagnostic agent. These structural features are not described or suggested by Seiver et al.

It can be seen, for example, that the magnetic particles in the present invention are of an order of magnitude smaller than the smallest magnetic particles described by Seiver et al. Thus, the lower limit for the particle size of the magnetic particles of Seiver et al of 10  $\mu\text{m}$  is 100 times larger than the largest magnetic particle contemplated by the present invention.

In the light of the foregoing, claim 1 is believed to distinguish over Seiver et al, and the rejection under 35 USC § 102 is believed to be fully overcome.

Claims 1, 2, and 6 to 10 are rejected under 35 USC § 102(a) as being anticipated by Veiga et al.

The Veiga et al document was submitted by the applicant. The document as submitted is in the form of a preprint prepared by the publisher for review by the authors. As such, the document which was submitted by the applicant in the Information Disclosure Statement was not the final published document. This can be seen from, for example, the designation of the publication which appears at the top of the first page of the document, namely, Carbohydrate Polymers 00 (1999) 000-000. The zeroes indicate the non-published state of the document.

The document was ultimately published as Carbohydrate Polymers 42 (2000) 353-357 (copy attached), in August 2000 and thus subsequent to applicant's priority date of April 19, 2000. Furthermore, the publication is a work of the inventors in the present application and dated less than twelve months before the filing date of the present application. As such, the publication is not a reference to the present application.

It is regretted that, in error, the unpublished preprint was submitted rather than the final published document.

Claims 1, 2, and 6 to 10 are rejected under 35 USC § 102(e) as being anticipated by Gunther et al.

Gunther et al teaches composite nanoparticles having a magnetic core provided with a coating of an oxidatively cleaved starch. Additionally, the nanoparticles preferably include a polymer coating, such as a functionalized polyalkylene oxide.

The nanoparticles are employed in magnetic resonance imaging, and the purpose of the starch and polymer coatings is to stabilize the particles and prolong the blood resonance time.

In the present invention, in the embodiment in which the matrix is derived from gelatinized starch granules, the composition does **not** comprise particles comprising a magnetic core and a coating of starch. Rather, in the present invention, in such embodiment, the particulate magnetic material is dispersed within the hydrogel matrix. Gunther et al has discrete particles, each particle having a core of magnetic material surrounded by a surface coating derived from starch. This is not a feature of the compositions of the present invention. In the present invention, the particulate material is not coated with starch. Rather, the magnetic particles are dispersed within the matrix which may be derived from starch.

Thus, claim 1 as amended is novel over Gunther et al. Furthermore, the area of utility as contemplated by claims 6 to 9 is unrelated to the area of utility described by Gunther et al. Gunther et al is not concerned with immuno-separation processes and is not concerned with diagnostic methods.

As set forth in claim 1, the matrix of the composition is permeable and has accessible interior surfaces defining a cage for physical or chemical entrapment of an immuno-reactant or diagnostic agent. Such a structure is clearly not part of Gunther et al which is directed to individual coated particles, and there is no teaching or suggestion of the "cage" structure for physical or chemical entrapment of an immuno-reactant or diagnostic agent.

In the light of the foregoing, reconsideration of the rejection under 35 USC 102 is requested.

Claim Rejections – 35 USC § 103

Claims 3 to 5 stand rejected under 35 USC § 103 as being unpatentable over Gunther et al.

Gunther et al has already been considered above. The analysis of Gunther et al appears to be based on hindsight after reading the specification of the present application. Nowhere does Gunther et al describe a cage structure for physical/chemical entrapment of antigens, antibodies, or anything else. The particles of Gunther et al are of an altogether different structure, each particle comprising a

Commissioner for Patents

Serial No. 09/837,742

core of magnetic material surrounded by a coating derived from starch. This is quite different from dispersion of magnetic particles within the matrix of a hydrogel as required by the present invention.

In Gunther et al the "gel" only exists as part of the manufacturing process of the magnetic particles. The procedure of Gunther et al involving the gel is well summarized at column 10, line 54 to column 11, line 1. Thus, in Gunther et al, ferrous and ferric salts and a base which are to produce the iron oxide particles are combined in a heated aqueous starch solution. The solution is allowed to cool so that it sets as a gel. The pH is adjusted, and the gel is treated with an oxidant which cleaves the starch and releases particles. These released particles are washed and filtered and optionally reacted with a polyalkylene oxide. Thereafter, the released particles are optionally sterilized.

The product of Gunther et al does not comprise magnetic particles dispersed within a hydrogel matrix, the matrix being permeable and having accessible interior surfaces defining a cage. The particles of Gunther et al are discrete magnetic particles, each having a surface coating of oxidized starch. The conjugation incidentally referred to by Gunther et al is evidently a chemical reaction between the targeting agent and the iron oxide core. The composite **particles** of Gunther et al are particularly described at column 8, lines 45 to 53, and it is clear from this and from all of the disclosure that the particles of Gunther et al comprise a magnetic core particle with a polymer coating material such as an oxidized starch coating.

In the light of the foregoing, reconsideration of the rejection under 35 USC § 103 is requested.

Concerning new claims 11 to 19, these are still further removed from Gunther et al in that they further define the immuno-separation and diagnostic method as well as the immuno-separation device. Gunther et al is not even concerned with such processes or devices and cannot possibly suggest these processes and devices.

In Gunther et al, the magnetic particles are the "active" agent in the magnetic resonance imaging as described in the background at column 1. In the present invention, they are the means of effecting separation of materials as part of an immuno-separation process or diagnostic method.

Favourable consideration of claims 11 to 19 is requested.

The foregoing represents a full response to the Office Action.

Commissioner for Patents

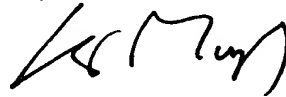
Serial No. 09/837,742

The application is believed to be in condition for allowance, and early and favourable action would be appreciated.

Respectfully,

ROBERT H. MARCHESSAULT ET AL

By:



Agent for the Applicant

Kevin P. Murphy

Regis. No. 26,674

OGILVY RENAULT

1981 McGill College Avenue

Suite 1600

Montreal, Quebec, Canada

H3A 2Y3

Tel. - (514) 847-4293

Enc.

## Formation and characterization of superparamagnetic cross-linked high amylose starch

V. Veiga<sup>a</sup>, D.H. Ryan<sup>b</sup>, E. Sourty<sup>a</sup>, F. Llanes<sup>c</sup>, R.H. Marchessault<sup>a,\*</sup>

<sup>a</sup>Pulp and Paper Research Center and Department of Chemistry, McGill University, Montreal, Canada, PQ H3A 2A7

<sup>b</sup>Department of Physics, McGill University, Montreal, Canada, PQ H3A 2A7

<sup>c</sup>Center of Biomaterials, University of Havana, Havana 10400, Cuba

Received 17 June 1999; received in revised form 4 October 1999; accepted 5 October 1999

### Abstract

A gelatinized cross-linked high amylose starch matrix with magnetic properties was synthesized via in situ formation of iron oxides inside the polymer matrix. Precipitation and multiple oxidation of ferrous ions were performed. The samples were observed using transmission and scanning electron microscopy, showing morphological changes in the magnetic and polymer phases. The iron content analysis revealed a decay from one oxidation cycle to the next one if no fresh ferrous solutions are added before the multiple oxidation. X-ray diffractograms, magnetization curves and Mössbauer spectra were also recorded for the characterization of the magnetic phase. The products exhibit superparamagnetic properties due to the presence of ferrimagnetic nanoparticles, although some other iron compounds are also present. © 2000 Elsevier Science Ltd. All rights reserved.

**Keywords:** Amylose; X-ray diffractograms; Mössbauer spectra

### 1. Introduction

Starch is one of the most widely used carbohydrate polymers and it is composed of two polysaccharides: linear amylose and branched amylopectin. Epichlorohydrin cross-linked high amylose starch, known by the commercial name of Contramid<sup>®</sup>, has been introduced as matrix for controlled drug release (Lenaerts, Dumoulin & Mateescu, 1991). Characterization of Contramid<sup>®</sup> has been described by Dumoulin, Alex, Szabo, Cartier and Mateescu (1998). Studies of the swelling profiles and drug release kinetics of Contramid<sup>®</sup> tablets under the influence of different chemical and physical variables have been reported (Moussa & Cartier, 1996, 1997). Recent progress in the use of this product as a drug excipient has been reviewed (Lenaerts et al., 1998).

The use of vinyl polymer particles with magnetic response in biochemistry and medicine has been described in several papers. The fields of application include not only drug delivery (Ugelstad, Mfutakamba, Mørk, Ellingsen & Berge, 1985), but also diagnostics and cell separation (Rembaun, Yen, Kempner & Ugelstad, 1982; Karlsson & Platt, 1991). By comparison, starch brings advantageous possibilities due to the presence of functional groups suitable for the coupling of different biological moieties at

the particle surfaces for immuno-based separations of antibodies. Some composite materials can be synthesized by coating finely divided magnetic iron oxides with natural or synthetic polymers, while in situ formation of the iron nanoparticles inside the polymers is also used. A review of these methods was published by Platsoucas (1987).

Since the Contramid<sup>®</sup> matrix is insoluble in water, an in situ method was selected to introduce magnetic properties into this starch excipient. Iron is introduced inside the Contramid<sup>®</sup> matrix by immersion in a ferrous chloride solution. Subsequently the iron is precipitated and finally oxidized. The use of this in situ synthesis method has been described (Sourty, Ryan & Marchessault, 1998) for magnetization of cellulosic gels which are non-ionic like Contramid<sup>®</sup>. The resulting superparamagnetic material was characterized using five techniques: X-ray diffraction, transmission (TEM) and scanning (SEM) electron microscopy, vibrating sample magnetometry and Mössbauer spectroscopy.

### 2. Materials and methods

#### 2.1. Materials

Contramid<sup>®</sup> powder, kindly supplied by Labopharm Inc.

\* Corresponding author.

BEST AVAILABLE COPY

BEST AVAILABLE COPY

(1200 boul. Chomedey, Laval, Quebec H7V 3Z3), was prepared using a patented process (Mateescu, Lenaerts & Dumoulin, 1991) based on epichlorohydrin cross-linking of high amylose starch (Hylon VII from National Starch) followed by purification and spray-drying from water to form a coarse powder. A solution of iron (II) chloride tetra hydrate (Aldrich Chemical Company, Inc.) was employed as iron source. Pellets of sodium hydroxide and hydrogen peroxide 30% solution (both from ACP Chemicals Inc.) were also used during the synthesis process.

## 2.2. *In situ* synthesis of the magnetic material

A suspension of 0.75 g of Contramid® in 25 ml of water (2.9 % (wt.) starch suspension) was slowly added to 250 ml of a degassed and constantly stirred 0.5 M solution of  $\text{FeCl}_4\text{H}_2\text{O}$ . The system was stirred, while keeping the  $\text{N}_2$  bubbling, for another 2 h. After this period the starch gel with entrapped ferrous ions was separated by centrifugation and dispersed in 250 ml of distilled water. Afterwards, 200 ml of a 0.5 M NaOH solution were added to the yellowish-brown starch solution, which immediately became greenish-brown. Finally, the mixture was placed into a  $65 \pm 5^\circ\text{C}$  water bath and 10 ml of hydrogen peroxide (10 % (wt.)) were added dropwise. The color became reddish-brown and, once the last drop added, the solution was removed from the heat source and stirred for 30 min. to complete the oxidation process. The final product was concentrated by centrifugation and the washed gel was either employed for further oxidation cycles or freeze-dried to a reddish-brown powder. More than one oxidation step implies the subsequent addition of the NaOH solution and the oxidation with  $\text{H}_2\text{O}_2$  solution. Five cycles were performed and the collected freeze-dried samples were characterized.

## 2.3. Determination of the iron content

Guelph Chemical Laboratories Ltd. (246 Silvercreek Parkway N., Guelph, Ontario N1H 1E7) provided the micro-analytical determination of the iron content for the samples obtained after the first, third and fifth cycles using a plasma technique.

## 2.4. X-ray diffraction

A Rigaku powder diffractometer with a Cu rotating anode generator and a graphite monochromator was used to analyze the products. Diffractometer scans as a function of the Bragg angle, as well as  $d$ -spacing were recorded.

## 2.5. Transmission electron microscopy

Aqueous dilute suspensions of the samples were applied and allowed to dry on Cu TEM grids, which were observed with a JEOL transmission electron microscope, model JEM2000X, operated at 80.0 kV for imaging by diffraction

contrast in the bright-field mode and also for selected area electron diffraction.

## 2.6. Scanning electron microscopy

The magnetic Contramid® powders were sprinkled on C-tapes and subsequently coated with Au/Pd using a Hummer VI Sputter Coater. The observations were performed with a JEOL JSM-840A scanning electron microscope. An acceleration voltage of 10.0 kV was applied in all cases.

## 2.7. Vibrating sample magnetometry

Approximately 20 mg of the different products at room temperature were vibrated in a magnetic field varying from  $-1.5$  to  $1.5$  T. The data of magnetization as a function of the applied field were plotted and employed for further calculations.

## 2.8. Mössbauer spectroscopy

Mössbauer spectra at room temperature were recorded with a conventional constant-acceleration spectrometer in transmission geometry and with a 1 GBq  $^{57}\text{CoRh}$  source. The spectra for the first, third and fifth cycles were obtained and fitted using a standard Mössbauer fitting program.

## 3. Results and discussion

According to the observed decrease of the iron content (42.56, 39.08 and 29.92% for the first, third and fifth cycle respectively) we can state that the iron compounds are not chemically bound to the polymer matrix. It seems that physical interactions between both components of the composite material are not strong enough to prevent the mechanical loss of magnetic phase when multiple oxidation cycles are performed. However, the iron content can be increased (51.30 and 52.05% for the third and fifth cycle respectively) when the magnetic starch gel is embedded in ferrous ions and the multiple oxidation is performed afterwards.

The X-ray diffraction patterns were very difficult to analyze since multiple iron compounds seem to be present and some peaks could correspond to more than one of them. Only the signals at  $2\theta = 35.09^\circ$  ( $d = 2.56 \text{ \AA}$ ) and  $2\theta = 62.82^\circ$  ( $d = 1.48 \text{ \AA}$ ) are constantly present in the diffractograms of the different cycles. They can be associated not only with magnetite ( $\text{Fe}_3\text{O}_4$ ) and maghemite ( $\gamma\text{-Fe}_2\text{O}_3$ ), very important in the final magnetic properties due to their high specific magnetizations, but also with other forms of iron oxides, such as haematite ( $\alpha\text{-Fe}_2\text{O}_3$ ). Oxyhydroxy products such as feroxyhite ( $\delta\text{-FeOOH}$ ) and lepidocrocite ( $\gamma\text{-FeOOH}$ ), are likely in the case of the first cycle. Additional peaks characteristic of the completely oxidized material appear only as a result of more than one oxidation step.

BEST AVAILABLE COPY

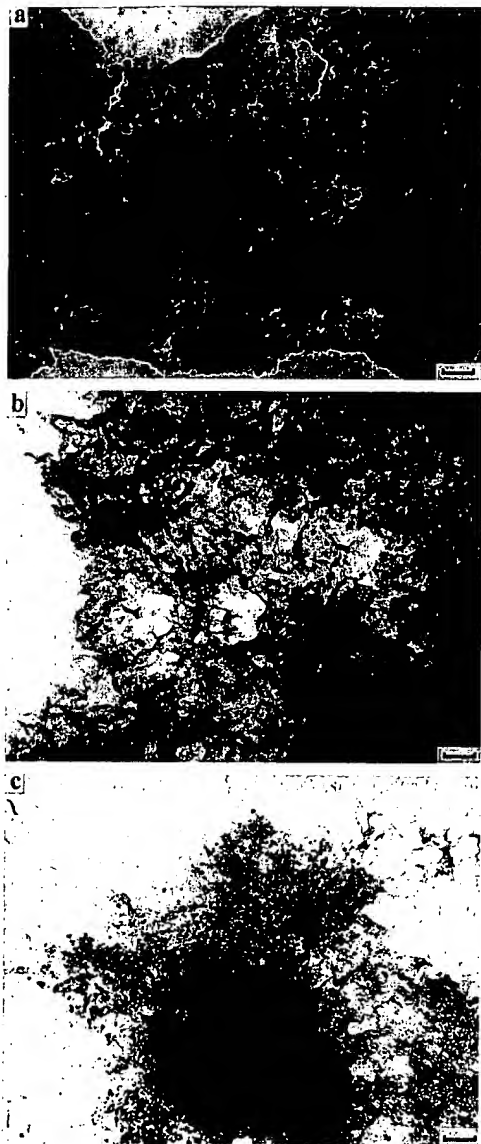


Fig. 1. TEM micrographs of the magnetic cross-linked high amylose starch after: (a) one; (b) three; and (c) five oxidation cycles. Scale bars are 100 nm (a) and 200 nm (b and c).

The above results were corroborated by the TEM micrographs showing nanoparticles with different shapes. After the first cycle a dark background of iron compounds with some larger domains, predominantly acicular up to 150 nm long, are observed (Fig. 1(a)). These exhibit powder

electron diffractograms corresponding to the ferroxhyte ( $\delta$ -FeOOH) phase, as reported by Powers (1975) under analogous conditions. Rounded particles with diameters close to 20 nm are prevalent with increase of the number of oxidation cycles, as seen in Fig. 1(b) and (c). Those dots can be associated principally with magnetite and maghemite.

Fig. 2(a) and (b) represent the SEM micrographs of the magnetic Contramid® after the third and fifth cycles respectively. Not only the shape of the magnetic phase but also the shape of the polymer surface changes from one cycle to another. Flaky polymer structures with needle-shaped protuberances and dots on the surface are clearly distinguished until the third cycle. The flakes could be a result of the freeze-drying procedures performed to obtain the powders. However, in the case of the fifth cycle a completely different composite morphology is observed. Needles are no longer present, while dots become predominant in a fairly clotty polymer matrix. These results agree with those obtained by TEM if we associate the needles and dots with the magnetic phase of the samples.

All samples showed good magnetic response under the influence of a permanent magnet; and the magnetization curves shown in Figs. 3 and 4 proved their superparamagnetism. High magnetizations, above  $6 \text{ J T}^{-1} \text{ kg}^{-1}$ , are present for relatively small magnetic field values, below  $0.5 \text{ T}$ , while neither coercivity nor remanence were observed. The saturation magnetization increases slightly from the first to the third cycle, despite the decreasing iron content. This can be explained by the chemical transformation occurring during the oxidation process, which leads to the conversion of some weakly ferrimagnetic or antiferromagnetic compounds (e.g. ferroxhyte or lepidocrocite) into strongly ferrimagnetic compounds (e.g. magnetite or maghemite). However, a decrease of the saturation magnetization is observed from the third to the fifth cycle, in agreement with the decrease of the iron content. This suggests that no more than three cycles should be performed in order to obtain a product with optimal magnetic properties, unless ferrous ions were constantly added to the system. In such a case the increase of the saturation magnetization is a direct result of the increase in the iron content.

The magnetization behavior allows to assume a simple model to estimate the size of the particles from the VSM data plotted in Fig. 4. The very small particles (smaller than the critical size) are considered as non-interacting ferrimagnetic domains with a certain size distribution. Their behavior resembles that of the classic paramagnetic gas and can be described by the Langevin function  $\mathcal{L}$  (Chikazumi, 1997):

$$M = M_s \sum_i \alpha_i \mathcal{L} \left( \frac{m_i V_i H}{kT} \right)$$

where  $M$  is the magnetization obtained for the applied magnetic field  $H$ ,  $M_s$  is the saturation magnetization, and

BEST AVAILABLE COPY



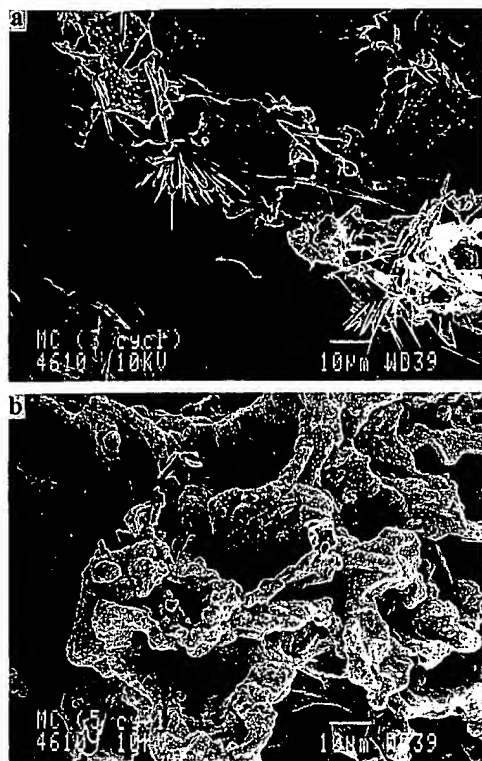


Fig. 2. SEM micrographs of the magnetic cross-linked high amylose starch after: (a) three and (b) five oxidation cycles.

$\alpha_i$  is the fraction of particles with volume  $V_i$  and specific spontaneous magnetization  $m_s$  at the temperature  $T$ .

Fig. 5 shows the size distribution curves obtained when assuming  $m_s = 5 \times 10^5 \text{ J T}^{-1} \text{ m}^{-3}$  (value for magnetite). The three cycles have similar distributions, principally for larger particle volumes. The chemical transformations

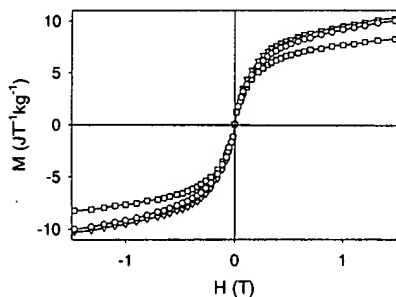


Fig. 3. Complete magnetization curves at room temperature for the samples after the first (○), third (▽) and fifth (□) oxidation cycle.

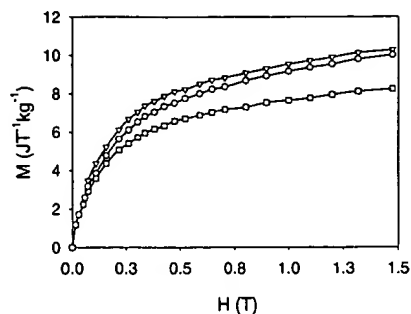


Fig. 4. Initial magnetization curves at room temperature for the samples after the first (○), third (▽) and fifth (□) oxidation cycle.

occurring during the consecutive oxidation cycles cause changes in the shapes of the particles, rather than changes in their sizes.

The volumes of the particles contributing to the VSM curves are lower than  $10^{-23} \text{ m}^3$ , which means that their diameters are lower than 27 nm if they are assumed as spherical. This value is slightly higher than the sizes observed by TEM. The initial parts of the magnetization curves of Fig. 4 are associated with the orientation of the largest particles at low applied fields and that is why the magnetization increases sharply. However, the model considered could lead to exaggerated estimates of the maximum volume since we are disregarding particle interactions and the orientation effect of the local particle fields, which are particularly important for small values of applied field and for particles with large volumes.

The products of the different cycles appear superparamagnetic on the time scale of the VSM measurements, i.e. about one second. Furthermore, particles are so small that the relaxation time for the change in magnetization direction is less than the lifetime of the nuclear excited state ( $\sim 10^{-7} \text{ s}$ ). As a consequence, the magnetic hyperfine splittings characteristic of the Mössbauer effect for the iron

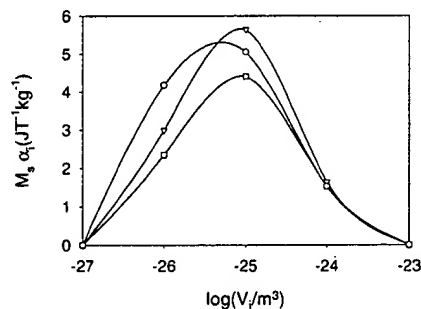


Fig. 5. Particle size distributions calculated from the VSM data for the first (○), third (▽) and fifth (□) oxidation cycle.

BEST AVAILABLE COPY

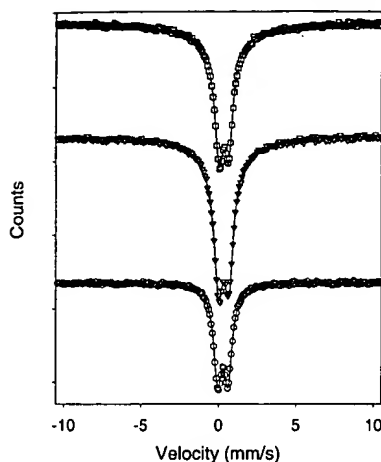


Fig. 6. Mössbauer spectra at room temperature for the samples after the first (○), third (▽) and fifth (□) oxidation cycle.

compounds are not observed, and the spectra collapse to doublet resonant peaks.

Fig. 6 illustrates the Mössbauer spectra for the three cycles studied. After the first oxidation process a doublet with a quadrupole splitting of  $\sim 0.68$  mm/s is observed. For the third and fifth cycles the quadrupole splittings were  $\sim 0.73$  and  $\sim 0.66$  mm/s, respectively. The differences are a result of the multiple iron compounds present in the samples.

#### 4. Conclusions

The proposed in situ synthesis of ferrites is an effective method to produce cross-linked high amylose starch with superparamagnetic properties, although it has been very difficult to control the oxidation process in order to obtain more selectively the optimal magnetic phases (magnetite and maghemite) in adequate proportions. Nevertheless, the magnetic behavior of the final products is appropriate for applications related to separation of bioactive molecules using molecular recognition methods.

The addition of fresh ferrous solutions on each oxidation cycle is recommended when an improvement in the overall magnetic response is desired. This modification increases

the iron content, thereby contributing to higher saturation magnetizations for each cycle.

#### Acknowledgements

The authors thank NSERC and Xerox for the financial support; David Coulon for the supporting technical work; and Dr Derek Gray for the stimulating discussions.

#### References

- Chikazumi, S. (1997). *Physics of ferromagnetism*, 2. (pp. 110–116). Oxford: Clarendon Press New York: Oxford University Press.
- Dumoulin, Y., Alex, S., Szabo, P., Carlier, L., & Mateescu, M. A. (1998). Cross-linked amylose as matrix for drug controlled release. X-ray and FT-IR structural analysis. *Carbohydrate Polymers*, 37, 361–370.
- Karlsson, G. B., & Platt, F. M. (1991). Analysis and isolation of human transferring receptor using the OKT-9 monoclonal antibody covalently crosslinked to magnetic beads. *Analytical Biochemistry*, 199, 219–222.
- Lenaerts, V., Dumoulin, Y., & Mateescu, M. A. (1991). Controlled release of theophylline from cross-linked amylose tablets. *Journal of Controlled Release*, 15, 39–46.
- Lenaerts, V., Moussa, I., Dumoulin, Y., Mebsout, F., Chouinard, F., Szabo, P., Mateescu, M. A., Carlier, L., & Marchessault, R. (1998). Cross-linked high amylose starch for controlled release of drugs: recent advances. *Journal of Controlled Release*, 53, 225–234.
- Mateescu, M. A., Lenaerts, V., & Dumoulin, Y. (1991). *Cross-linked material for controlled-release of biologically active compounds*, US Patent 618, 650.
- Moussa, I. S., & Carlier, L. H. (1996). Characterization of moving fronts in cross-linked amylose matrices by image analysis. *Journal of Controlled Release*, 42, 47–55.
- Moussa, I. S., & Carlier, L. H. (1997). Evaluation of cross-linked amylose press-coated tablets for sustained drug delivery. *International Journal of Pharmacology*, 149, 139–149.
- Platsoucas, C. D. (1987). In M. S. El-Asser & R. M. Fitch (Eds.), *Future directions in polymer colloids*, NATO ASI Series, Series E: Applied Science, 138. Dordrecht: N. Nijhoff Publ.
- Powers, D. A. (1975). *Magnetic behavior of basic Iron (III) compounds*. PhD thesis, California Institute of Technology, Pasadena, CA, USA.
- Rembaun, A., Yen, R. C. K., Kempner, D. H., & Ugelstad, J. (1982). Cell labelling and magnetic separation by means of immunoreagents based on polyacrolein microspheres. *Journal of Immunological Methods*, 52, 341–351.
- Sourty, E., Ryan, D. H., & Marchessault, R. H. (1998). Ferrite-loaded membranes of microfibrillar bacterial cellulose prepared by in situ precipitation. *Chemical Materials*, 10, 1755–1757.
- Ugelstad, J., Mfutakamba, H. R., Mark, P. C., Ellingsen, T., & Berge, A. (1985). Preparation and application of monodisperse polymer particles. *Journal of Polymer Science: Polymer Symposium*, 72, 225–240.

BEST AVAILABLE COPY

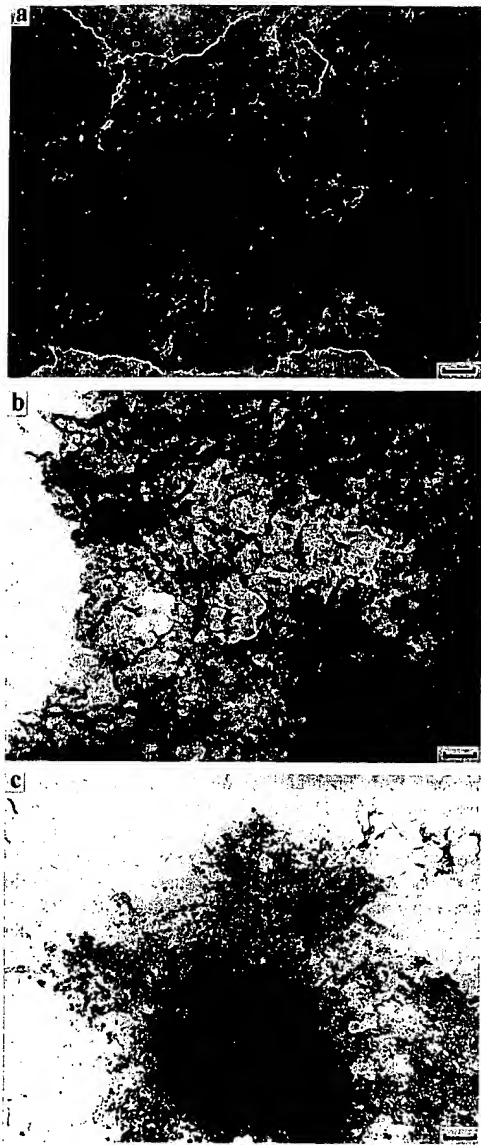


Fig. 1. TEM micrographs of the magnetic cross-linked high amylose starch after: (a) one; (b) three; and (c) five oxidation cycles. Scale bars are 100 nm (a) and 200 nm (b and c).

The above results were corroborated by the TEM micrographs showing nanoparticles with different shapes. After the first cycle a dark background of iron compounds with some larger domains, predominantly acicular up to 150 nm long, are observed (Fig. 1(a)). These exhibit powder

electron diffractograms corresponding to the feroxyhite ( $\delta$ -FeOOH) phase, as reported by Powers (1975) under analogous conditions. Rounded particles with diameters close to 20 nm are prevalent with increase of the number of oxidation cycles, as seen in Fig. 1(b) and (c). Those dots can be associated principally with magnetite and maghemite.

Fig. 2(a) and (b) represent the SEM micrographs of the magnetic Contramid<sup>®</sup> after the third and fifth cycles respectively. Not only the shape of the magnetic phase but also the shape of the polymer surface changes from one cycle to another. Flaky polymer structures with needle-shaped protuberances and dots on the surface are clearly distinguished until the third cycle. The flakes could be a result of the freeze-drying procedures performed to obtain the powders. However, in the case of the fifth cycle a completely different composite morphology is observed. Needles are no longer present, while dots become predominant in a fairly clotty polymer matrix. These results agree with those obtained by TEM if we associate the needles and dots with the magnetic phase of the samples.

All samples showed good magnetic response under the influence of a permanent magnet; and the magnetization curves shown in Figs. 3 and 4 proved their superparamagnetism. High magnetizations, above  $6 \text{ J T}^{-1} \text{ kg}^{-1}$ , are present for relatively small magnetic field values, below 0.5 T, while neither coercitivity nor remanence were observed. The saturation magnetization increases slightly from the first to the third cycle, despite the decreasing iron content. This can be explained by the chemical transformation occurring during the oxidation process, which leads to the conversion of some weakly ferrimagnetic or antiferromagnetic compounds (e.g. feroxyhite or lepidocrocite) into strongly ferrimagnetic compounds (e.g. magnetite or maghemite). However, a decrease of the saturation magnetization is observed from the third to the fifth cycle, in agreement with the decrease of the iron content. This suggests that no more than three cycles should be performed in order to obtain a product with optimal magnetic properties, unless ferrous ions were constantly added to the system. In such a case the increase of the saturation magnetization is a direct result of the increase in the iron content.

The magnetization behavior allows to assume a simple model to estimate the size of the particles from the VSM data plotted in Fig. 4. The very small particles (smaller than the critical size) are considered as non-interacting ferrimagnetic domains with a certain size distribution. Their behavior resembles that of the classic paramagnetic gas and can be described by the Langevin function  $\mathcal{L}$  (Chikazumi, 1997):

$$M = M_s \sum_i \alpha_i \mathcal{L} \left( \frac{m_i V_i H}{kT} \right)$$

where  $M$  is the magnetization obtained for the applied magnetic field  $H$ ,  $M_s$  is the saturation magnetization, and

BEST AVAILABLE COPY